SPE 112976

Understanding the Rate of Clean Up for Oil Zones after a Gel Treatment

R.S. Seright, SPE, New Mexico Petroleum Recovery Research Center, W. Brent Lindquist, SPE, and Rong Cai, Stony Brook University

This paper was prepared for presentation at the 2008 SPE Improved Oil Recovery Symposium held in Tulsa, Oklahoma, U.S.A., 19–23 April 2008.

Abstract

In our previous work, X-ray computed microtomography (XMT) was used to establish why pore-filling Cr(III)-acetate-HPAM gels reduced permeability to water much more than to oil. Our results suggest that permeability to water was reduced to low values because water must flow through gel itself, whereas oil pressing on the gel in a porous medium forced pathways by dehydration—leading to relatively high permeability to oil. Those studies involved obtaining 3D pore-level X-ray images at the saturation endpoints—for example, after forcing 20 pore volumes of oil or water through the core following gel placement.

The dependence of oil permeability on oil throughput determines how long it takes for a production well to "clean up" or restore productivity after a gel treatment. Consequently, we were interested in how the gel dehydration process progresses as a function of oil throughput. This paper describes a new study where pore-scale XMT images were obtained at a variety of oil (hexadecane) throughput values after gel placement (involving a pore-filling Cr(III)-acetate-HPAM gel). For each pore in our image volume, we followed oil and water saturations as a function of oil throughput. These studies were performed both in water-wet Berea sandstone and in hydrophobic porous polyethylene. In hydrophobic porous polyethylene, oil saturations increased and gel was destroyed (presumably dehydrated) quite quickly in the smallest pores (10^{-6} mm^3). Also, oil saturations increased and gel was destroyed quickly in the largest pores (<0.005 mm^3). In contrast, oil saturations rose much more gradually for the most common or intermediate-sized pores (around 10^{-4} mm^3, the peak in the pore size distribution). The minimum in oil saturation versus pore size may result from a balance between gel dehydration by oil film growth versus gel extrusion. Presumably, during oil injection after gel placement, an oil film forms with a thickness that is about the same on all polyethylene surfaces. However, because the ratio of film thickness to pore or throat size increases with decreased pore size, gel dehydration occurs faster and more effectively in the smallest polyethylene pores, causing oil saturation to increase with decreased pore size. This effect may lose its signicance for pore sizes above 10^{-4} mm^3. As pore size increases above 10^{-4} mm^3, gel extrusion from the pore becomes more likely—explaining why oil saturation increased with increased pore size for the largest pores.

In contrast in water-wet Berea sandstone, increases in oil saturation occurred evenly over all pore sizes (10^{-6} to 0.02 mm^3) for all oil throughput values. Consistent with imbibition and drainage studies performed before gel placement, oil apparently had equal access to Berea pores of all sizes, and thus uniformly dehydrated gel in pores of all sizes. Gel extrusion did not appear to be significant in the Berea pores.

Introduction

An ability of gels to reduce permeability to water much more than that to oil is critical for successful applications of gel treatments in production wells if hydrocarbon zones are not protected during gel placement (Liang 1993, Sydansk 2007). If gelant penetrates into an oil zone and gel forms, some time will be required before the oil penetrates through the gel bank and significant restoration of permeability to oil can occur (Seright 2006a, 2006b). The dependence of oil permeability on oil throughput determines how long it takes for a production well to "clean up" or restore productivity after a gel treatment. **Figs. 1 and 2** illustrate throughput dependence of water and oil for two core experiments—one using a hydrophobic porous polyethylene core (8.1 darcy initial permeability) and the other using a strongly water-wet Berea sandstone core (356 md initial permeability). Both cores were initially filled with gel that contained 0.5% Alcoflood 935 HPAM, 0.0417% Cr(III) acetate, 1% NaCl, and 0.1% $CaCl_2$. Neither core contained oil before saturation with gel. After gel formation in the cores, water (brine with 1% NaCl and 0.1% $CaCl_2$) was injected first, resulting in stable permeabilities of 60 μd in the polyethylene core (solid circles in Fig. 1) and 15 μd in the Berea core (solid diamonds in Fig. 2). These permeabilities translate to water

residual resistance factors (F_{rrw} or permeability reduction values) of 135,000 in porous polyethylene and 23,730 in Berea. If this gel is positioned in a water zone, permeability to water should be permanently reduced to very low values (e.g., 15 to 60 μd).

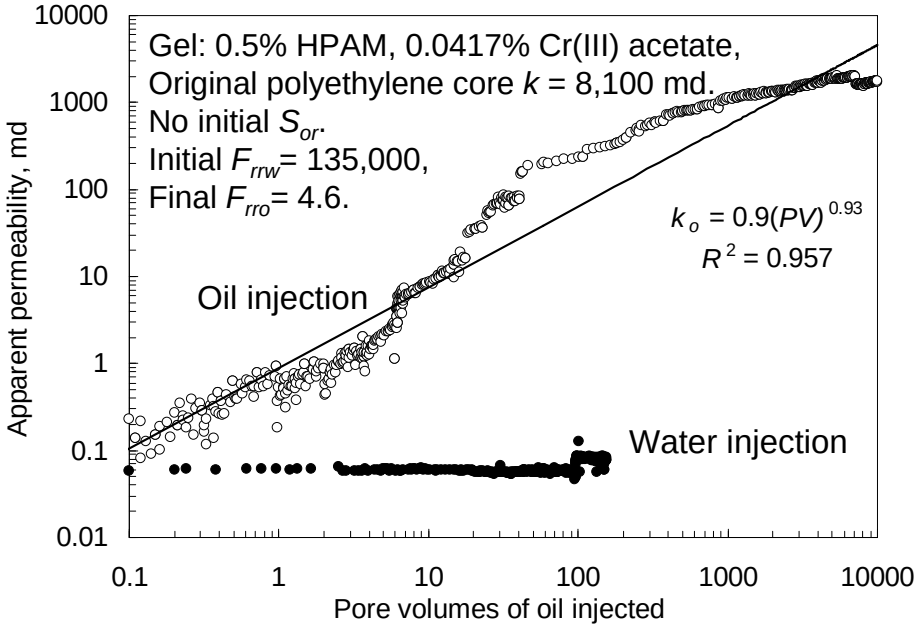

Fig. 1—Permeabilities to water and oil after gel placement in a polyethylene core.

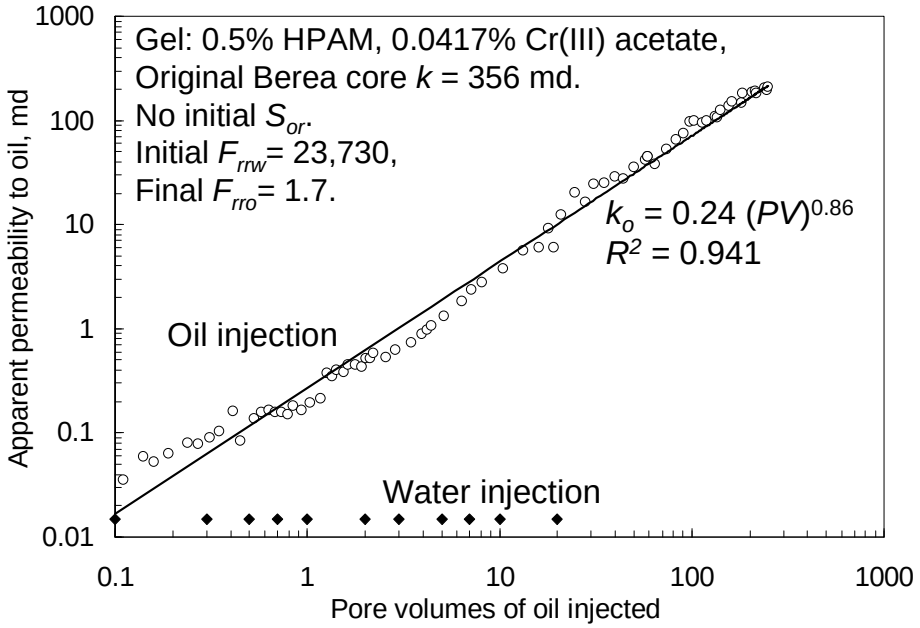

Fig. 2—Permeabilities to water and oil after gel placement in a Berea sandstone core.

In contrast to the behavior during water flow, permeability to oil (k_o) rises steadily during the course of injecting many pore volumes (PV) of oil (open circles in Figs. 1 and 2). The rise in k_o was described by Eq. 1 in porous polyethylene and by Eq. 2 in Berea sandstone.

$$k_o = 0.9\, PV^{0.93} \quad \text{.....(1)}$$

$$k_o = 0.24\, PV^{0.86} \quad \text{.....(2)}$$

The exponents in these equations indicate that the increase in permeability to oil was nearly linearly proportional to oil throughput. At the end of oil injection (after 300-10,000 *PV* of oil), the oil residual resistance factor (F_{rro} or permeability reduction factor) was 1.7 in Berea and 4.6 in porous polyethylene. This observation demonstrates the extent to which oil flow can compromise the gel in oil zones.

This study uses X-ray computed microtomography (XMT) to understand the throughput dependence of oil permeability after a gel treatment. First, we briefly review the XMT method. Second, we describe the pore structure of Berea sandstone and porous polyethylene. Third, we characterize fluid saturations on a pore level at the oil and water saturation endpoints. Fourth, we describe fluid saturations as a function of oil and water throughput in Berea and polyethylene with no gel present.. Next, we review our existing view for the pore-level mechanism that is responsible for disproportionate permeability reduction provided by pore-filling gels. Finally, we describe fluid saturations as a function of pore size and oil throughput after gel placement.

The XMT Method

In this paper, we describe imaging experiments using high-resolution computed X-ray microtomography to compare the oil and water pathways and fluid distributions at various stages before and after gel treatment. We used the ExxonMobil beamline X2-B at the National Synchrotron Light Source (Flannery et al. 1987, Dunsmuir et al. 1991, Seright et al. 2002, 2003, 2006c). To avoid end effects, imaging was performed within a 6.5-mm diameter, 3.25-mm long segment of each core centrally located along its 30 mm length. Depending on the experiment, voxel resolution was from 4.1 to 4.93 μm and the total image volume was from 29 to 50.5 mm^3. Image analysis typically focused on a 450x450x475 voxel region of each image. The 3DMA-Rock software package was used to analyze the image sequences. Its segmentation algorithm, based upon indicator kriging, was used to segregate grain/void space in the first image in each sequence, and to separate oil/water phases within the pore space in each subsequent image. Details of these procedures and analytical methods can be found in our previous references (Lindquist et al. 1996, Seright et al. 2006c, Prodanovic et al. 2006, 2007).

Core Properties

We used Berea sandstone and porous polyethylene as core materials (Seright et al. 2006c). The Berea cores had permeabilities of 0.3 to 0.5 darcys and a porosity of 0.2. The polyethylene cores had permeabilities of 8 to 10 darcys and a porosity of 0.4. Wettability tests produced Amott-Harvey indexes of 0.7 for the brine (1% NaCl, 0.1% $CaCl_2$)/oil (hexadecane)/Berea sandstone system and –0.8 for the brine/oil/porous polyethylene system—confirming the water-wet character of Berea sandstone and the oil-wet character of porous polyethylene. Based on XMT analysis, **Fig. 3** compares the pore size distributions for 0.47-darcy Berea sandstone and 8.8-darcy porous polyethylene.The average pore size for polyethylene (0.00052 mm^3) was 44% greater than that for Berea (0.00035 mm^3). Interestingly, the median pore size was greater for Berea (0.00016 mm^3) than for polyethylene (0.00010 mm^3). The higher average for polyethylene occurred because it contained a larger fraction of pores with sizes greater than 0.002 mm^3 (compare the high end of the distributions in Fig. 3). Incidentally, if the pores were spherical (which they are not), the average pore radius would be 50 μm for polyethylene and 44 μm for Berea.

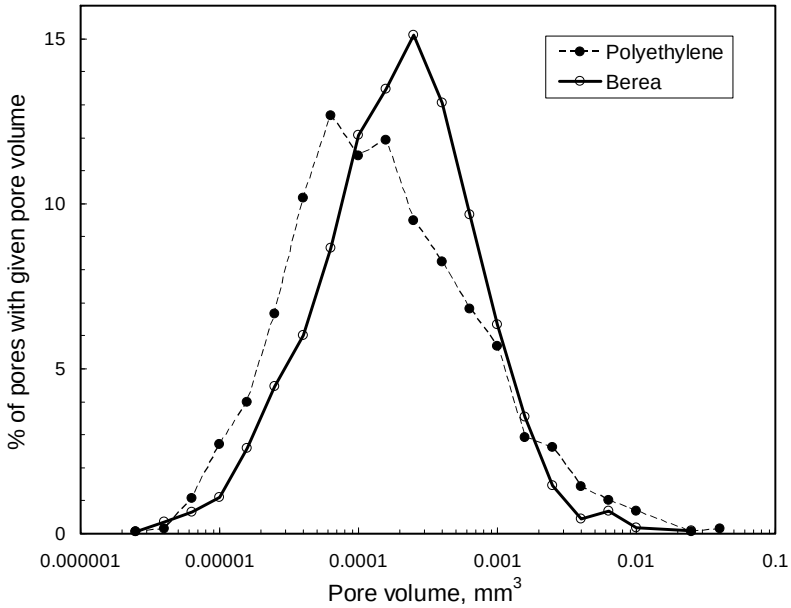

Fig. 3—Pore size distributions for Berea sandstone and porous polyethylene.

Upon first consideration of the similar pore size distributions for the two materials (Fig. 3), it may seem surprising that the polyethylene cores are 18.7 times more permeable than the Berea cores (Table 1). The capillary bundle model of porous media can be used to explain the observations. This model relates the average pore size (d_p) to the permeability (k) and porosity (ϕ).

$$d_p \propto [(1-\phi)/\phi]\,(k/\phi)^{0.5} \quad \text{.....(3)}$$

The ratio, d_p / {[(1-ϕ)/ ϕ] (k / ϕ)$^{0.5}$}, is 50 (0.4)/[(1-0.4) (8.8/0.4)$^{0.5}$] or 7.11 for porous polyethylene and is 44 (0.2)/[(1-0.2)(0.47/0.2)$^{0.5}$] or 7.18 for Berea sandstone. These calculations suggest that the large permeability difference between the two porous media can be attributed to the differences in porosity.

Table 1 provides a summary of the core properties (Seright et al. 2002, 2006c, Prodanovic et al. 2006, 2007). The average pore throat area was 1,400 μm^2 for the Berea sandstone and 1,630 μm^2 for the porous polyethylene. The average pore throat radius (assuming circular throat areas) was 11 μm for Berea and 11.4 μm for polyethylene. The aspect ratio can be defined as the effective pore radius divided by the effective throat radius. (The effective pore radius computed is for a sphere with a volume equivalent to that measured for the pore. The effective throat radius computed is for a circle with an area equivalent to that measured for the throat.) As shown in Table 1, the average aspect ratio was about 4 for both Berea and polyethylene. The distribution of aspect ratios was also similar for the two porous media. As pore volume increased from 10^{-5} mm^3 (effective pore radius ~13 μm) to 0.002 mm^3 (effective pore radius ~78 μm), the average aspect ratio increased steadily from 2 to 6. For a given pore size, a wide range of aspect ratios were noted. For all cores at a given pore size, the standard deviation (of aspect ratios) was typically 65% of the mean value.

Table 1—Summary of Core Properties

Property	Berea sandstone	Porous polyethylene
Wettability	Water-wet	Oil-wet
Permeability	0.47 darcys	8.8 darcys
Porosity	0.2	0.4
Average pore radius	44 μm	50 μm
Average throat radius	11 μm	11.4 μm
Ave. body/throat aspect ratio	4.0	4.4
Average coordination number	4	6

The average coordination number was 4 for Berea sandstone and 6 for porous polyethylene (Seright et al. 2002). (The coordination number is the number of exits from a pore.) For the smallest pores, the coordination number was around three for both types of cores. As the pore size increased, the coordination numbers increased—with the polyethylene core experiencing a slightly more rapid increase than the Berea cores. For a given pore size, standard deviations were typically 20% to 40% of the mean values. For Berea sandstone, our results were reasonably consistent with those reported by Ioannidis et al. 1997, who performed analyses based photomicrographs of 78 serial sections through a double pore cast of a Berea sample.

A wide range of pore sizes and shapes were observed in both types of porous media (Prodanovic 2006). The pore volume and surface area distributions for Berea sandstone and porous polyethylene were qualitiatively similar. For each pore, three orthogonal diameters can be assigned to the pore space: one for the larger diameter, one for the smaller diameter, and one for the middle diameter. Considering all pores, a wide range of pore dimensions were noted. However, on average, the larger diameter was 1.6 times greater than the middle diameter, which in turn, was 1.6 times greater than the smaller diameter. The smaller pore diameter was most characteristic of the effective pore radius for flow.

A wide range of pore throat sizes and shapes were also noted in both types of porous media (Prodanovic 2006). For each throat, two orthogonal diameters can be assigned: one for the larger diameter and one for the smaller diameter. Considering all throats, on average, the larger diameter was 1.6 times greater than the smaller diameter.

Imbibition and Drainage before Gel Placement

In previous work (Seright et al. 2002, 3003, 2006c, Prodanovic et al. 2006, 2007), we obtained XMT images and analysis for Berea and polyethyelene cores at endpoint saturations of oil (hexadecane) and brine (with 1% NaCl, 0.1% $CaCl_2$) before gel placement. Comparison between drainage and imbibition in both porous media before gel placement provided an interesting insight into conventional wisdom.

Oil Drainage from Oil-Wet Polyethylene: Fluid Saturations Were Consistent with Conventional Wisdom.

When a wetting phase drains from a porous medium, conventional wisdom argues that the smallest pores should retain the highest wetting-phase saturation. This expectation is consistent with our findings after water injection into (oil drainage from) oil-wet porous polyethylene (**Fig. 4**). After the first drainage displacement (to residual oil saturation or S_{or}), oil saturation in the imaged region of the polyethylene core was 14%. As expected, the average oil (wetting phase) saturation in the smallest

detected pores was more than 80% while the medium to large pores were more likely to be filled with water. During a second cycle of oil drainage (i.e., a second waterflood to drive the core to S_{or} after an intervening oil flood), most large pores again filled almost completely with water, while most small pores retained high oil saturations (Seright et al. 2006c).

Oil Imbibition into Polyethylene: Oil Was Immobile in Small Polyethylene Pores.
As mentioned, at S_{or}, most small pores had nearly 100% oil saturation, while most large pores had nearly 100% water saturation (Fig. 4). When oil was injected to drive the core to residual water saturation, S_{wr}, water was displaced from most medium to large pores so that most pores ended with nearly 100% oil saturation (**Fig. 5**). Thus, consistent with conventional wisdom, the wetting phase was largely immobile in small polyethylene pores.

Water Drainage from Berea: The Saturation Distribution Deviated from Conventional Wisdom.
In Berea sandstone, at connate water saturation (S_{wr}) before gel placement, S_w in the imaged region was 16%. The water saturations at S_{wr} are plotted in **Fig. 6** for each of the pores in the Berea sample volume. At S_{wr}, 54.5% of the pores had S_w < 5%; water saturations near zero were common for pores in most size ranges. Water saturations in the smallest pores were scattered over the entire range from 0 to 100%—just as in most other size ranges (Seright 2006c). A calculation using the Young-LaPlace equation confirmed that oil should readily be able to enter the smallest pores (~10^{-5} mm^3) in our Berea cores (Seright et al. 2002).

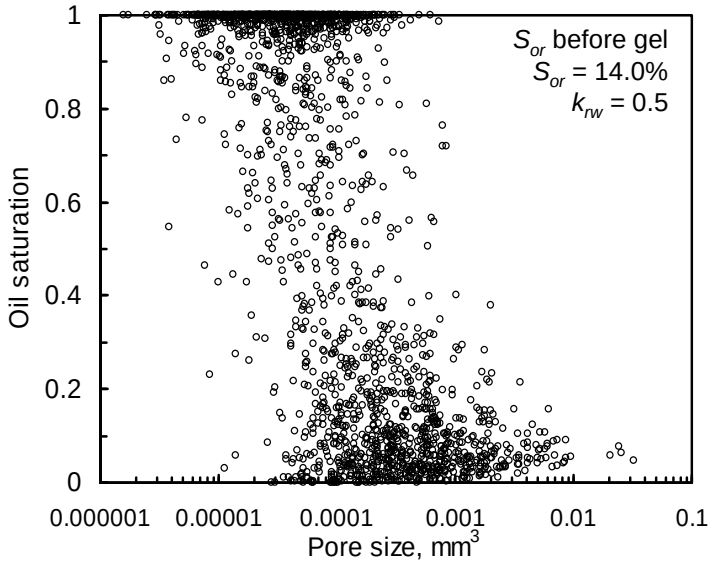

Fig. 4—Polyethylene @ S_o before gel.

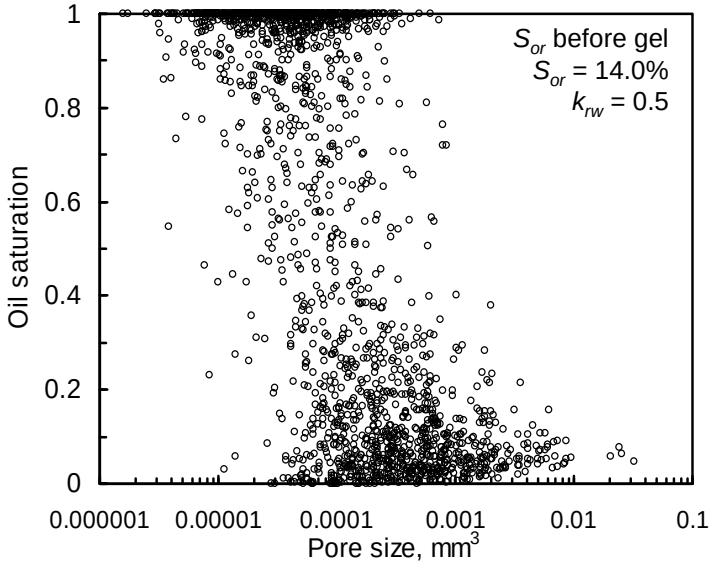

Fig. 5—Polyethylene @ S_{wr} before gel.

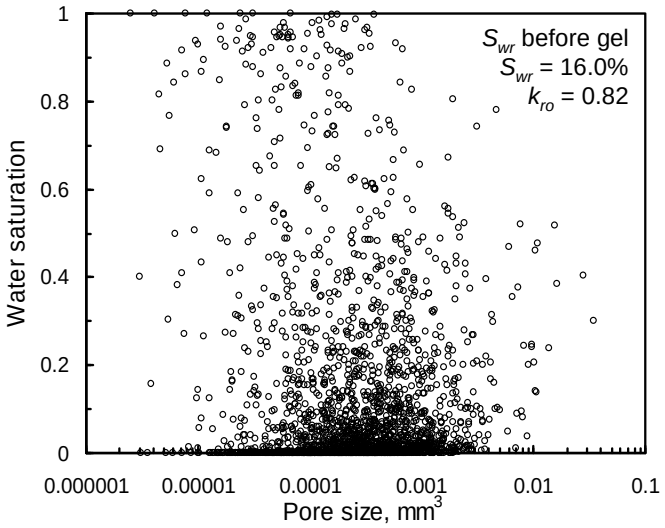

Fig. 6—Berea @ S_{wr} before gel.

On first consideration, this finding appears to contradict the expectation that the water saturations approach 100% in the smallest pores of a water-wet porous medium. The work of Dullien et al. (1989) helps to explain the behavior that we see in Berea and why it deviates from that in polyethylene. Berea pores are typically coated with kaolinite that significantly increases the surface roughness of the pore walls. In contrast, the pore walls in polyethylene are quite smooth. Scanning electron microscope images of the two samples are shown in **Fig. 7**. At S_{or}, after oil drainage from the smooth polyethylene pore walls, an extremely thin (nanometer scale) oil film may have coated most pore walls (or possibly, no film may remain). At S_{wr} in water-wet Berea, the rough clay coating made the effective thickness of the water film much greater than for any oil film in porous polyethylene. With a thicker effective wetting film, water drained fairly efficiently from the smallest detected Berea pores when oil was injected—thus allowing the smallest detected pores to reach water saturations comparable to those in larger pores. In contrast, when water was injected into porous polyethylene, oil usually became hydraulically isolated in the smallest detected pores because any remaining wetting film was too thin to efficiently drain oil. Consequently, high oil saturations were usually seen in the smallest detected polyethylene pores. The important message here is that for the pore sizes involved with our porous media, access to pores (through effective films) is at least as important in determing residual saturations as capillary pressure, interfacial tension, or applied pressure gradient.

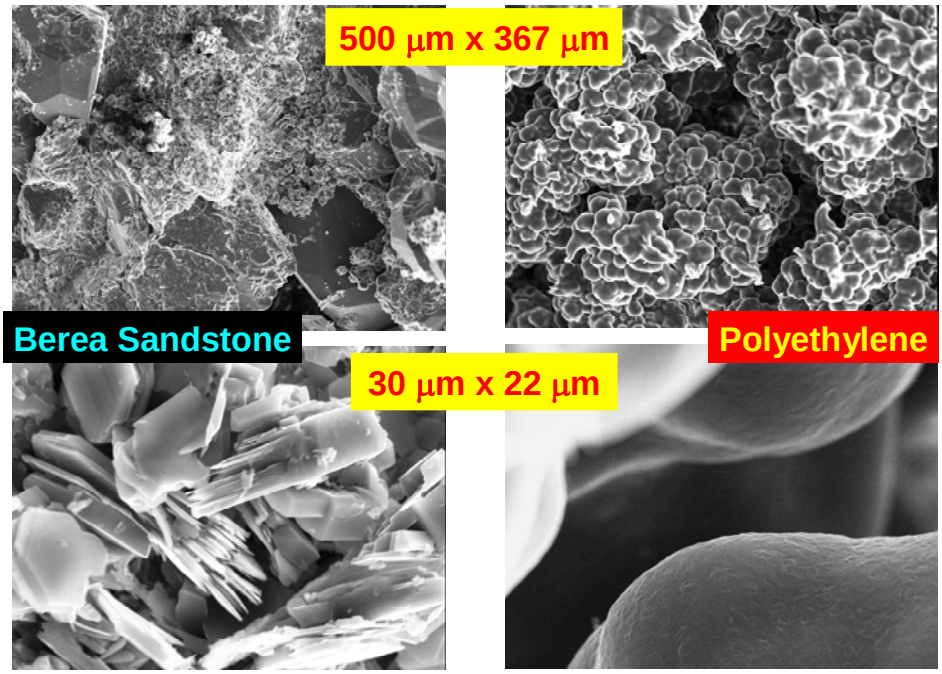

Fig. 7—Electron micrographs of Berea sandstone and porous polyethylene.

Water Imbibition into Berea: Saturation Changes Were Insensitive to Berea Pore Size.
Water saturation at S_{or} in the imaged region in Berea was 81.6%. The average pore saturation was not sensitive to pore size. For all size ranges, note the large number of pores with high water saturations; 39.4% of the pores had $S_w > 95\%$. During the transition from S_{wr} to S_{or} in Berea (**Fig. 8**), pores in all detected size ranges experienced significant gains in water saturation (averaging 65.6%). Pore size did not appear to significantly influence the extent of the transition (Seright et al. 2006c).

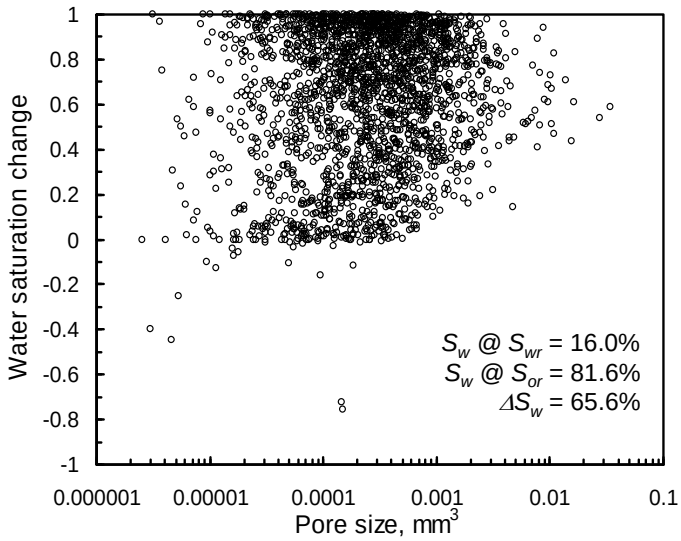

Fig. 8—Changes in Berea: S_{wr} to S_{or}.

Connectivity of Phases before Gel Placement.
Analysis of the connectivity of the fluid phases produced results that were consistent with expectations and with previous work (Chatzis et al. 1983, Seright et al. 2006c). A summary of findings (in both Berea and porous polyethylene) include the following:

1. Before gel placement, at least 97.9% of the injected phase (oil or water) was connected.
2. Before gel placement, most residual non-wetting blobs were "singlets"—i.e., isolated within individual pores.
3. Changes in blob connectivity qualitatively followed the trends expected from the saturation changes. The largest oil blob always grew when the oil saturation increased and shrank when the oil saturation decreased. Similarly, the largest water blob always grew when the water saturation increased and shrank when the water saturation decreased.

Fig. 9 utilizes the ability to identify single pores and fluid blobs to examine changing fluid occupation within a single Berea pore. The grain surface of the pore is shown as a (partially transparent) gray mesh surface. The pore has coordination number 4, and the view into the pore is through one channel entrance. The red blobs show the position of oil within the pore at residual oil conditions (S_{or} before gel). The green blobs show the position of water in the pore at residudal water conditions (S_{wr} before gel). The positioning of the blobs in this pore follows conventional wisdom—with the residual oil residing more in the pore center and residual water lying along the pore surface.

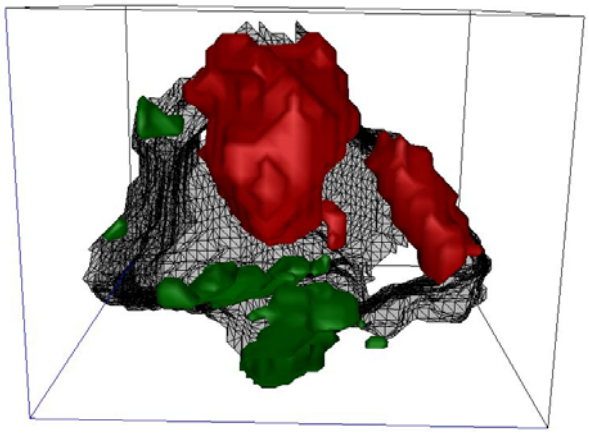

Fig. 9—Measured positioning of residual fluid phases [oil at S_{or} (red) and water at S_{wr} (green)] tends to follow conventional wisdom in this Berea pore (Seright et al. 2006c).

Imbibition and Drainage as a Function of Throughput before Gel Placement

We also studied oil and water saturations in pores as a function of water and oil throughput in porous polyethylene cores (Prodanovic et al. 2006). In porous polyethylene, the residual wetting phase (oil) does not move much during either imbibition or drainage. During the course of injecting 64.5 pore volumes of water into porous polyethylene, less than 10% of the pores that contained the original residual oil saturation experienced a significant satuation change. Similarly during oil injection (imbibition), less than 10% of these same pores experienced a significant saturation change. Also, during steady-state fractional flow of oil/water ratios of 90:10, 80:20, and 50:50, less than 7% of the pores that contained the original residual oil saturation experienced a significant satuation change.

In contrast, 60-70% of the residual non-wetting phase (water) moves during both imbibition and drainage. After many pore volumes of oil flow, XMT identified pores that contained the residual non-wetting phase (water) in porous polyethylene. During subsequent water injection, we followed saturation changes in these pores at water throughput values of 0.54, 1.08, 1.61, 2.69, 5.38, 10.8, and 64.5 pore volumes. At 0.54 *PV*, significant saturation changes were noted in 57% of the pores that contained the original residual water saturation. Even with a favorable mobility ratio, it takes up to 10 *PV* for the residual non-wetting phase to stabilize.

These studies showed that during drainage (water injection into porous polyethylene), the non-wetting phase (water) filled the largest pores first (solid symbols in **Fig. 10**). During imbibition (oil injection), water leaves the largest pores last (open symbols in Fig. 10). For cases where fractional flow was fixed, water saturations tended to decrease with decreased pore size (Prodanovic 2006).

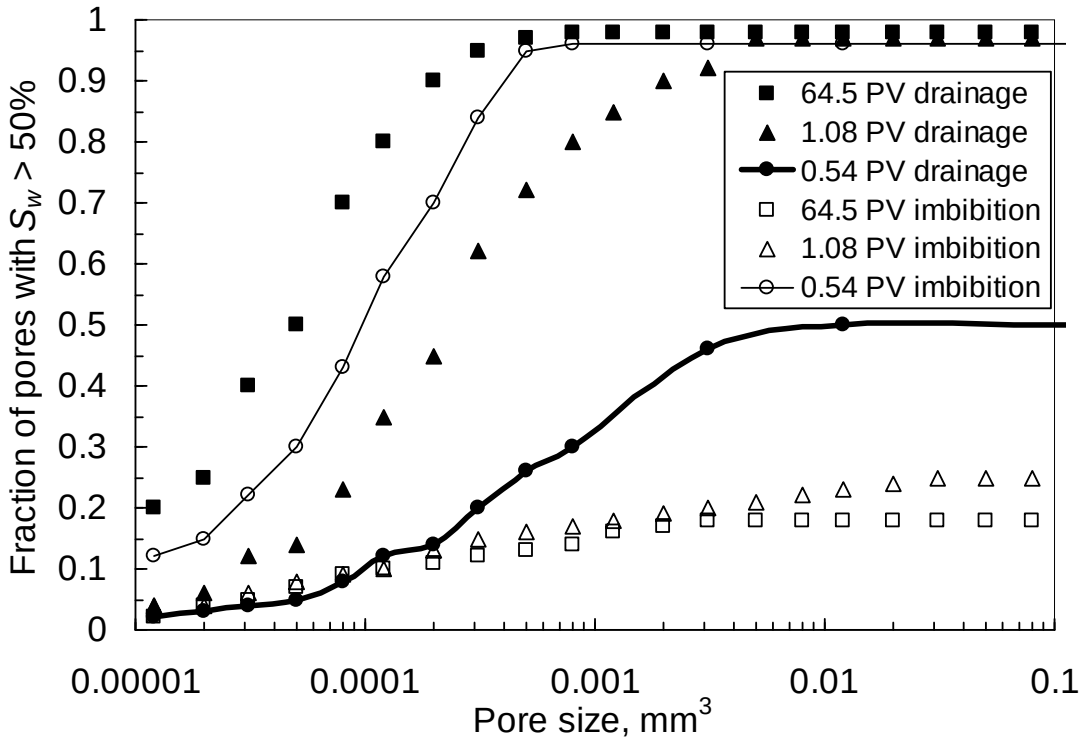

Fig. 10—Fraction of polyethylene pores with water saturation above 50% vs pore size and fluid throughput.

Current Mechanistic View for Disproportionate Permeability Reduction by Pore-Filling Gels

This section summarizes our current views of the mechanism for disproportionate permeability reduction for pore-filling gels such as Cr(III)-acetate-HPAM.

Water Flow after Gel Placement.

Immediately after placement and gelation, the water-based gel occupies all of the aqueous pore space. Residual oil may be trapped in pore centers in water-wet rock such as Berea (see the schematic in **Fig. 11**). In oil-wet porous media (e.g., porous polyethylene), low mobility "residual oil" may coat pore walls. With either wetting condition, if water or brine is injected after gel placement, it must flow through the gel itself. Since the inherent permeability to water is in the microdarcy range for flow through the gel, a very large permeability reduction is observed (Seright 1993). For rock with an initial permeability (before gel) around one darcy, the water residual resistance factor can be greater than 10,000. Thus, the gel can greatly reduce flow from gel-invaded water zones.

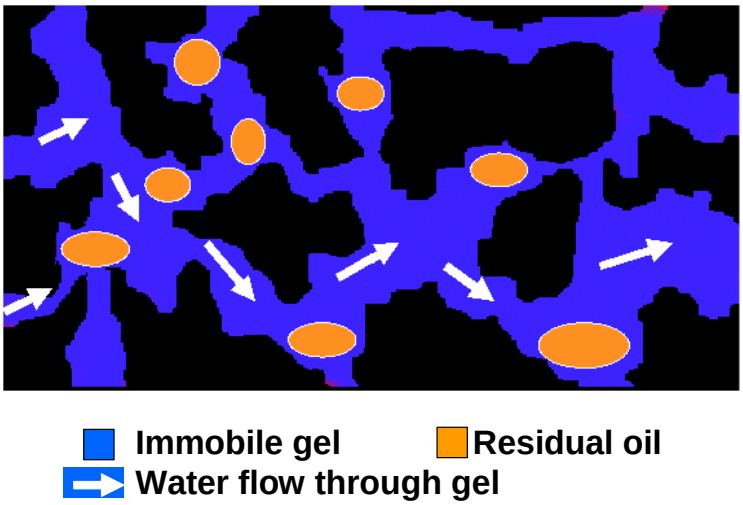

Fig. 11—Water must flow *through* the gel (Seright et al 2006c).

Oil Flow after Gel Placement.

Oil is typically the first fluid that contacts the gel-treated region when a well is returned to production. We found that oil flow reduces the pore volume occupied by gel. This volume reduction created pathways for oil flow, thus restoring an important level of permeability to oil. The schematic in **Fig. 12** illustrates this process.

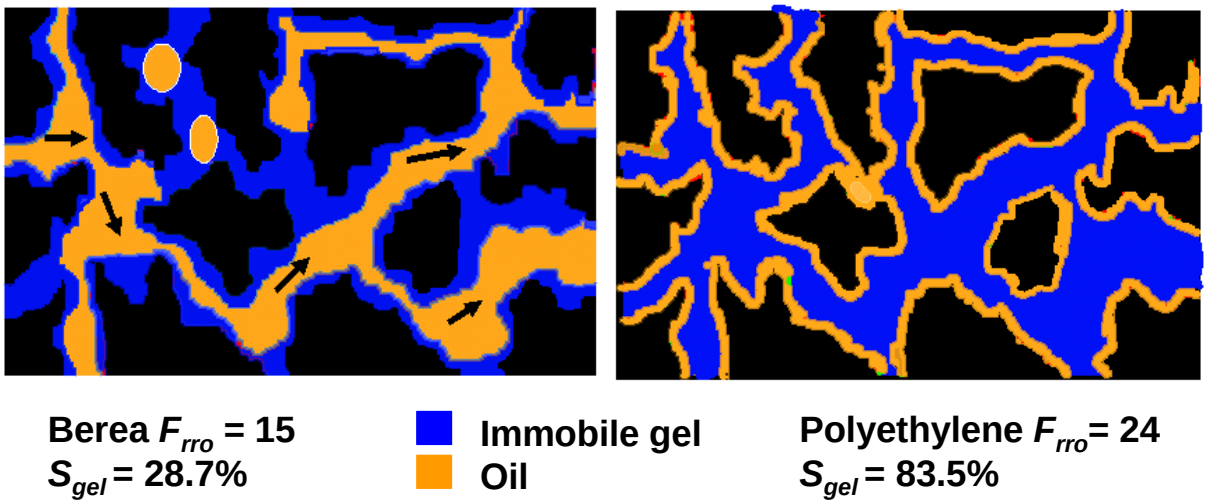

Fig. 12—Oil opens pathways by dehydrating the gel (Seright et al. 2006c).

When oil is injected, how does a reduction in gel volume occur? Several possibilities come to mind, including oil (a) ripping through the gel, (b) concentrating or dehydrating the gel, (c) mobilizing the gel, or (d) chemically destroying the gel. As our oil (hexadecane) was not reactive with any of the gel, brine, or rock components, possibility d), chemical destruction of the gel, does not seem likely. Our analysis supports the dehydration mechanism in Berea sandstone and porous polyethylene over the ripping or gel mobilization mechanisms (Seright et al. 2006c). In particular, the apparent reduction in gel saturation during oil injection was insensitive to pore size in Berea and was greatest in small pores in porous polyethylene. If ripping or gel mobilization were the dominant mechanisms, losses in gel volume should have been greatest in the largest pores. To explain, if gel failure (i.e., ripping or gel extrusion) occurred at a gel-rock interface or within the gel, force balance analysis suggests that the pressure gradient for gel failure should be inversely proportional to the pore radius (Zaitoun and Bertin 1996, Liu and Seright 2001). Thus, for a given applied pressure gradient, gel failure should occur dominantly in larger pores. Since this did not occur, our results argue against the ripping or gel mobilization mechanisms. In contrast, the observed XMT results could be consistent with the dehydration mechanism. With a fixed pressure gradient applied through the porous medium, gel in all pores could be "squeezed" or dehydrated to the same extent, regardless of pore size. In very permeable sand packs, data from other researchers supports ripping or extrusion mechanisms for creating oil pathways (Seright et al. 2006c, Nguyen et al. 2006).

Imbibition and Drainage as a Function of Throughput after Gel Placement

Our XMT previous studies that were performed after gel placement obtained images at the saturation endpoints—for example, after forcing 20 pore volumes of oil or water through the core after gel placement (Seright et al. 2002, 2003, 2006c). The dependence of oil permeability on oil throughput determines how long it takes for a production well to "clean up" or restore productivity after a gel treatment (Seright 2006a, 2006b). Consequently, we were interested in how the gel dehydration process progresses as a function of oil throughput. We were particularly interested in whether oil paths develop preferentially in large pores versus small pores. To answer this question, we saturated a polyethylene core (8 darcy original permeability) and a Berea sandstone core (328 md original permeability) with a Cr(III)-acetate-HPAM gelant and allowed the gel to form. This gel contained 0.5% Ciba Alcoflood 935™ HPAM, 0.0417% Cr(III) acetate, 1% NaCl, and 0.1% $CaCl_2$.

Average saturations in the XMT Image Volume.

Fig. 13 plots the average saturations in the XMT image volume as a function of *PV* of oil injected. One surprising aspect of the results was that the average saturation from the XMT data was noticeably greater than expected from the oil throughput data. For example, in the polyethylene core, the average oil saturation in the image volume reached 54% after injecting only 0.2 *PV* of oil. Also, in the Berea sandstone core, the average oil saturation in the image volume reached 77% after injecting only 0.1 *PV* of oil. On first consideration, these findings do not seem possible. One would expect that the average oil saturation in the core could not exceed 10% after injecting 0.1 *PV* of oil and 20% after injecting 0.2 *PV* of oil. However, remember that the saturations were measured *in the image volume*. The image volume was only 12 mm^3 in the center of a 1,300 mm^3 core. The mobility ratio was extremely high during oil flow through the gel. A finger of oil could reach a given location within the core with a very small throughput. Consequently, it is quite possible that the image volume may be flooded to high oil saturation at an earlier time than the average for the core. By the same logic, it is possible that the oil fingers might completely miss the image volume, so that oil saturations remain low until very high throughput values. Thus, some degree of "luck" or random chance led to the particular saturations levels seen in Fig. 13. Nonetheless, within a given image volume, the distribution of oil in small, medium, and large pores is of interest.

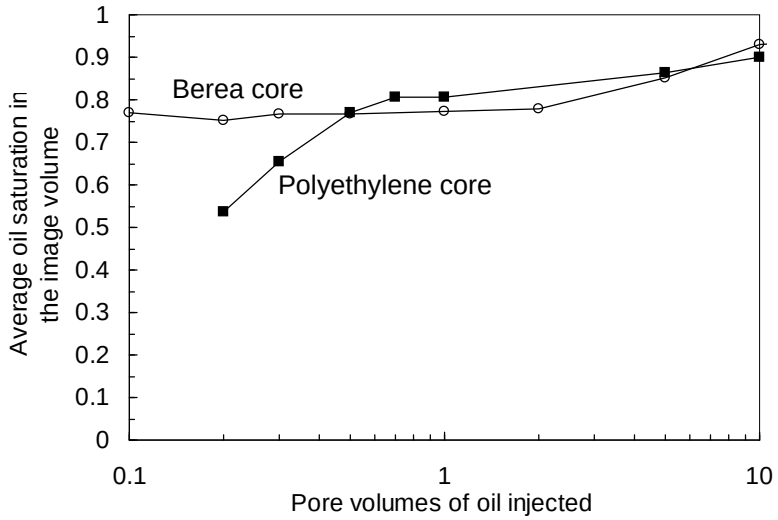

Fig. 13—Average oil saturations in the image volumes versus oil throughput.

XMT Results for the Polyethylene Core.

The distribution of oil saturations as a function of pore size and oil throughput in the image volume of the polyethylene core is shown in **Fig. 14**. For all throughput values, a minimum in oil saturation was observed for pore sizes around $5x10^{-5}$ – 10^{-4} mm^3. (The oil saturation minimum moved to slightly lower pore sizes with increased oil throughput—from $6x10^{-5}$ mm^3 at 0.2 *PV* to $4x10^{-5}$ mm^3 at 10 *PV*.) The smallest polyethylene pores (10^{-6}-10^{-5} mm^3) filled rapidly with oil. Oil saturations jumped to almost 60% in these pores after injecting only 0.2 *PV* of oil. We speculate that the hydrophobic polyethylene pore walls provided an effective conduit to imbibe oil through the porous medium. Presumably, growth of an oil film on the pore walls led to compression of the gel. This compression forced a small amount of water to flow through the gel structure to the outlet end of the core (i.e., gel dehydration). Also presumably, this slight loss of water caused a small increase in concentration of polymer within the gel (Seright et al. 2006c).

In contrast, oil saturations rose much more gradually for the most common or intermediate-sized pores. For pores with sizes around $5x10^{-5}$ mm^3, oil saturations were 0.24 at 0.2 *PV*, 0.38 at 1 *PV*, and 0.64 *PV* at 5 *PV*. Conceivably, the slower rise in oil saturations could be responsible for the gradual increase in k_o shown in Fig. 1. There are so many pores within the size

range around $5x10^{-5} – 10^{-4}$ mm^3 that the oil *must* flow through these pores in order to get through the core. Thus, these pores provide the critical resistance that determines the overall permeability.

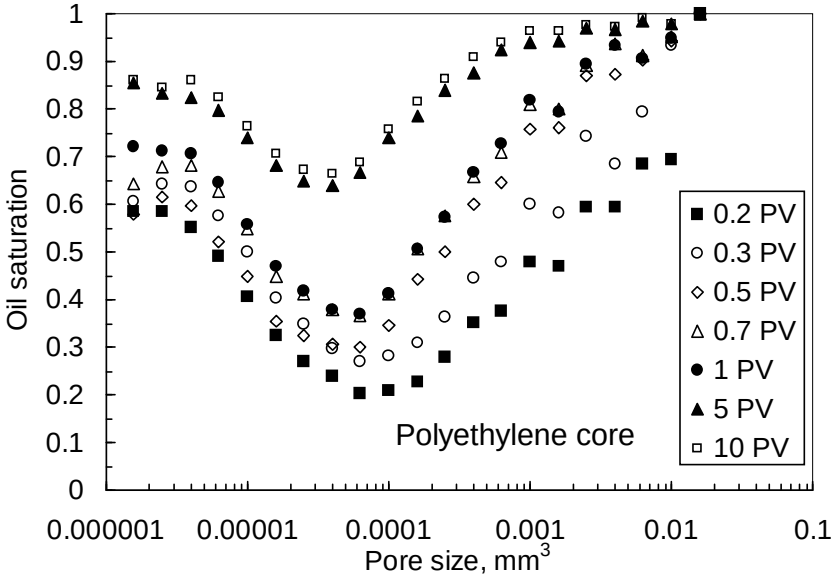

Fig. 14—Oil saturation versus pore size and oil throughput: polyethylene core.

The largest pores also filled quite rapidly with oil. For pores larger than 0.0063 mm^3 (accounting for 61% of the total pore space in the image volume), the oil saturation was over 90% after injecting only 0.3 *PV*. Although it is possible that gel dehydration was responsible for the gains in oil saturation in these pores, we are inclined to believe that ripping or gel extrusion were more likely the responsible mechanism. We note that in sand packs with permeabilities comparable to our polyethylene core, data from the University of Kansas supports ripping or extrusion mechanisms for creating oil pathways (Seright et al. 2006c, Nguyen et al. 2006). The hydrophobic polyethylene surface probably allowed a film of oil to penetrate into all pores, where it could act as a lubrication layer to facilitate gel extrusion from the pore. Gel extrusion most likely occurs in the largest pores, thus explaining why the oil saturation in Fig. 14 increased with increased pore size above 10^{-4} mm^3. No gel was physically observed extruding from the cores. However, it is quite possible that any extruded gel was too small and too dilute to notice visually.

Consequently, the minimum in oil saturation versus pore size in Fig.14 may result from a balance between gel dehydration by oil film growth versus gel extrusion. Presumably, the oil film thickness is about the same on all polyethylene surfaces. However, because the ratio of film thickness to pore or throat size increases with decreased pore size, gel dehydration occurs faster and more effectively in the smallest polyethylene pores, causing oil saturation to decrease with increased pore size (left side of Fig. 14). Presumably, this effect loses significance for pore sizes above 10^{-4} mm^3. As pore size increases above 10^{-4} mm^3, gel extrusion from the pore becomes more likely—explaining why oil saturation increased with increased pore size for the right side of Fig. 14.

XMT Results for the Berea Core.

The distribution of oil saturations as a function of pore size and oil throughput in the Berea sandstone core are shown in **Fig. 15**. For any given oil throughput, the oil saturation was fairly independent of pore size. Why did the smallest Berea pores not experience large increases in oil saturation, as was observed in the polyethylene core? Presumably, the answer is that the water-wet Berea rock had no propensity to imbibe oil, so no oil film formed and grew as we suggested for the hydrophobic polyethylene. Why did the largest Berea pores not show large increases in oil saturation, as was observed in the polyethylene core? The porosity of the Berea rock was about half that for polyethylene. Perhaps, the ripping and extrusion mechanisms were more prevalent in the high-porosity polyethylene. Also, in polyethylene, perhaps the oil film promoted (through lubrication) gel extrusion from the largest pores. In Berea, this oil film probably was not present. Instead consistent with imbibition and drainage studies performed before gel placement in Berea, oil apparently had equal access to Berea pores of all sizes, and thus uniformly dehydrated gel in pores of all sizes. Gel extrusion did not appear to be significant in the Berea pores.

Interestingly, the average oil satuation jumped to about 0.75 in Berea after injection of only 0.1 *PV* of oil (Fig. 15). In contrast, in porous polyethylene, an oil saturation of 0.75 had not been reached in the mid-sized pores until injection of 10 *PV* of oil (Fig. 14). The rate of increase in oil permeability was roughly the same for the two porous media (compare Figs. 1 and 2). Apparently, in water-wet Berea, the remaining gel (after dehydration) was positioned to more effectively restrict oil flow (i.e., perhaps in or near pore throats) than was the case for the hydrophobic porous polyethylene. Perhaps, inducing a

wettability reversal might enhance the rate of clean up after a gel treatment in water-wet rock. On the other hand, it is also possible that the jump in oil saturation from 0 to 0.75 was not directly related to the extended rate of increase in oil permeability seen in Fig. 2. As mentioned earlier, the gradual increase in k_o show in Figs. 1 and 2 were attributed to the unstable displacement associated with viscous fingering or wormholing (Seright 2006a, 2006b). The rapid jump in oil saturation in Berea between 0 and 0.1 *PV* may have occurred simply because the oil finger fortuitously swept the imaged volume. In contrast, in polyethylene, the small image volume apparently was swept less rapidly (see the left side of Fig. 13).

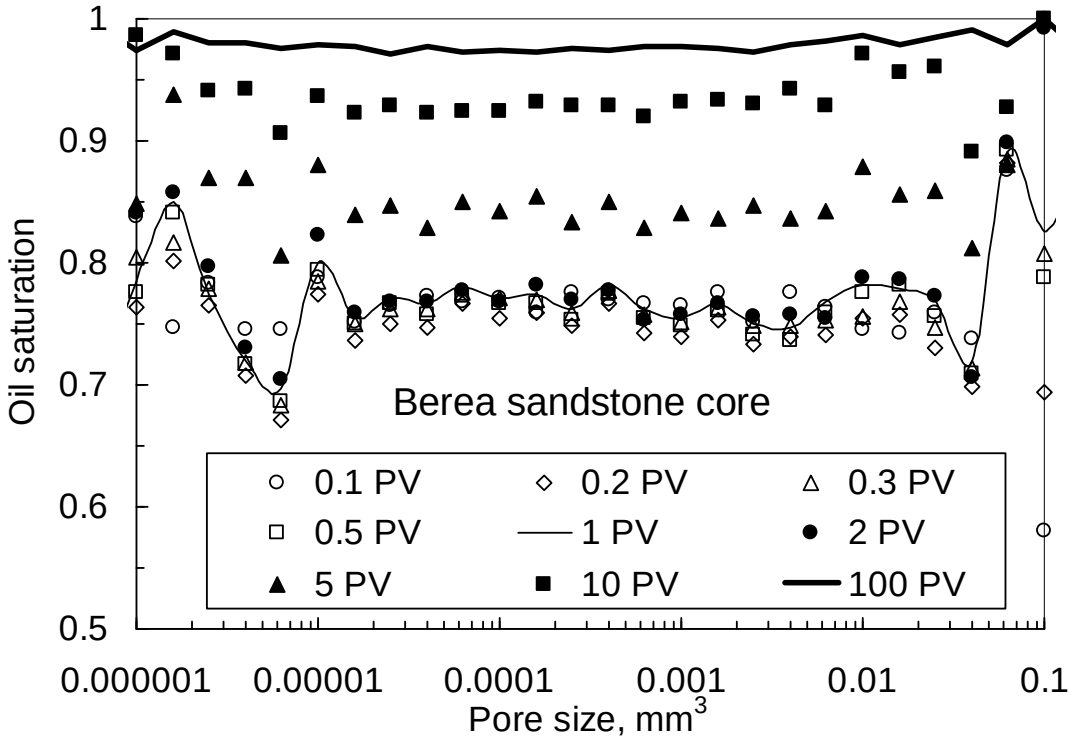

Fig. 15—Oil saturation versus pore size and oil throughput: Berea core.

Conclusions

To understand the rate of oil clean up after a gel treatment, pore-scale XMT images were obtained at a variety of oil (hexadecane) throughput values after gel placement (involving a pore-filling Cr(III)-acetate-HPAM gel). For each pore in our image volume, we followed oil and water saturations as a function of oil throughput. These studies were performed both in water-wet Berea sandstone and in hydrophobic porous polyethylene.

1. In hydrophobic porous polyethylene, oil saturations increased and gel was destroyed (presumably dehydrated) quite quickly in the smallest pores (10^{-6} mm^3). Also, oil saturations increased and gel was destroyed quickly in the largest pores (<0.005 mm^3). In contrast, oil saturations rose much more gradually for the most common or intermediate-sized pores (around $5x10^{-5}$ – 10^{-4} mm^3, the peak in the pore size distribution). The minimum in oil saturation versus pore size may result from a balance between gel dehydration by oil film growth versus gel extrusion.

2. In contrast in water-wet Berea sandstone, increases in oil saturation occurred evenly over all pore sizes (10^{-6} to 0.02 mm^3) for all oil throughput values. Consistent with imbibition and drainage studies performed before gel placement, oil apparently had equal access to Berea pores of all sizes, and thus uniformly dehydrated gel in pores of all sizes. Gel extrusion did not appear to be significant in the Berea pores.

Acknowledgements

We gratefully acknowledge ConocoPhillips, ExxonMobil, and Marathon for financial support of this work. This research was carried out in part at the National Synchrotron Light Source, Brookhaven National Laboratory, which is supported by the U.S. Department of Energy, Division of Materials Sciences and Division of Chemical Sciences. We are also grateful to John Dunsmuir and ExxonMobil for use of beamline X2-B.

Nomenclature

d_p = average pore size, μm

F_{rr} = residual resistance factor (permeability before/after gel placement)
F_{rro} = residual resistance factor for oil
F_{rrw} = residual resistance factor for water
k = permeability, darcys [μm^2]
k_{gel} = inherent permeability of gel to water, darcys [μm^2]
k_o = permeability to oil, darcys [μm^2]
k_{ro} = relative permeability to oil
k_{rw} = relative permeability to water
k_w = permeability to water, darcys [μm^2]
PV = pore volumes of fluid injected
R = correlation coefficient
S_o = oil saturation
S_{or} = residual oil saturation
S_w = water saturation
S_{wr} = residual water saturation
ϕ = porosity

References

Chatzis, I., Morrow, N.R., and Lim, H.T. 1983: "Magnitude and Detailed Structure of Residual Oil Saturation," *SPEJ*, 311-326.

Dullien, F.A.L. et al. 1989: "The Effects of Surface Roughness on the Capillary Pressure Curves and the Heights of Capillary Rise in Glass Bead Packs," *J. Colloid Interf. Sci.*, **127**, 362-372.

Dunsmuir, J.H., et al. 1991: "X—Ray Microtomography: A New Tool for the Characterization of Porous Media," paper SPE 22860 presented at the SPE Annual Technical Conference and Exhibition, Dallas, TX, Oct. 6-9.

Flannery, B.P., et al. 1987: "Three-Dimensional X—Ray Microtomography," *Science*, **237**, 1439.

Ioannidis, M.A. et al. 1997: "Comprehensive Pore Structure Characterization Using 3D Computer Reconstruction and Stochastic Modeling," paper SPE 38713, presented at the SPE Annual Technical Conference and Exhibition, San Antonio, TX, Oct. 5-8.

Liang, J., Lee, R.L., and Seright, R.S. 1993: "Placement of Gels in Production Wells," S*PEPF*, 276-284; *Transactions* AIME 295.

Lindquist, W.B., Lee, S.M., Coker, D.A., Jones, K.W., and Spanne, P. 1996: "Medial Axis Analysis of Void Structure in Three-Dimensional Tomographic Images of Porous Media," *J. Geophys. Res.*, **101**, 8297-8310.

Liu, J., and Seright, R.S. 2001: "Rheology of Gels Used For Conformance Control in Fractures," *SPEJ*, 120-125.

Nguyen, T.Q., et al. 2006: "Effects of Gelant Composition and Pressure Gradients of Water and Oil on Disproportionate Permeability Reduction of Sandpacks Treated With Polyacrylamide-Chromium Acetate Gels," *SPEJ* 145-157.

Prodanovic, M., Lindquist, W.B., and Seright, R.S. 2006: "Porous Structure and Fluid Partitioning in Polyethylene Cores from 3D X-ray Microtomographic Imaging," *J. Colloid and Interface Science*, **298,** 282-297.

Prodanovic, M., Lindquist, W.B., and Seright, R.S. 2007: "3D Image-Based Characterization of Fluid Displacement in a Berea Core," Advances in Water Resources, **30,** 214-226.

Seright, R.S. 1993: "Effect of Rock Permeability on Gel Performance in Fluid-Diversion Applications," In Situ, **17**, 363-386.

Seright, R.S, Liang J., Lindquist, W.B., and Dunsmuir, J.H. 2002: "Characterizing Disproportionate Permeability Reduction Using Synchrotron X-Ray Computed Microtomography," *SPEREE*, 355-364.

Seright, R.S., Liang, J., Lindquist, W.B., and Dunsmuir, J.H. 2003: "Use of X-Ray Computed Microtomography to Understand Why Gels Reduce Permeability to Water More Than That to Oil," *J. Petroleum Science and Engineering*, **39**(3-4), 217-230.

Seright, R.S. 2006a: "Clean Up of Oil Zones after a Gel Treatment," *SPEPO*, 237-244.

Seright, R.S. 2006b: "Optimizing Disproportionate Permeability Reduction," paper SPE 99443 presented at the SPE/DOE Symposium on Improved Oil Recovery, Tulsa, OK, April 22-26.

Seright, R.S., Prodanovic, M., and Lindquist, W.B. 2006c: "X-Ray Computed Microtomography Studies of Fluid Partitioning in Drainage and Imbibition Before and After Gel Placement: Disproportionate Permeability Reduction," *SPEJ*, 159-170.

Sydansk, R.D., and Seright, R.S. 2007: “When and Where Relative Permeability Modification Water-Shutoff Treatments Can Be Successfully Applied,” *SPEPO*, 236-247.

Zaitoun, A. and Bertin, H. 1996: “Two-Phase Flow Property Modifications by Polymer Adsorption,” paper SPE 39631 presented at the SPE/DOE Improved Oil Recovery Symposium, Tulsa, OK, April 19-22.